Supplementary Information

Electrochemical lithiation of the layered superionic conductors $AgCrSe_2$ and $CuCrSe_2$

Seongbak Moon,[1] Md Towhidur Rahman,[3] Noah P. Holzapfel,[1] Alexandra Zevalkink,[2] & Veronica Augustyn[1*]

[1] Department of Materials Science and Engineering
North Carolina State University
Raleigh, NC 27695 (USA)

[2] Department of Chemical Engineering and Materials Science
Michigan State University
East Lansing, MI 48824 (USA)

[3] Department of Mechanical Engineering
Michigan State University
East Lansing, MI 48824 (USA)

* corresponding author e-mail: vaugust@ncsu.edu

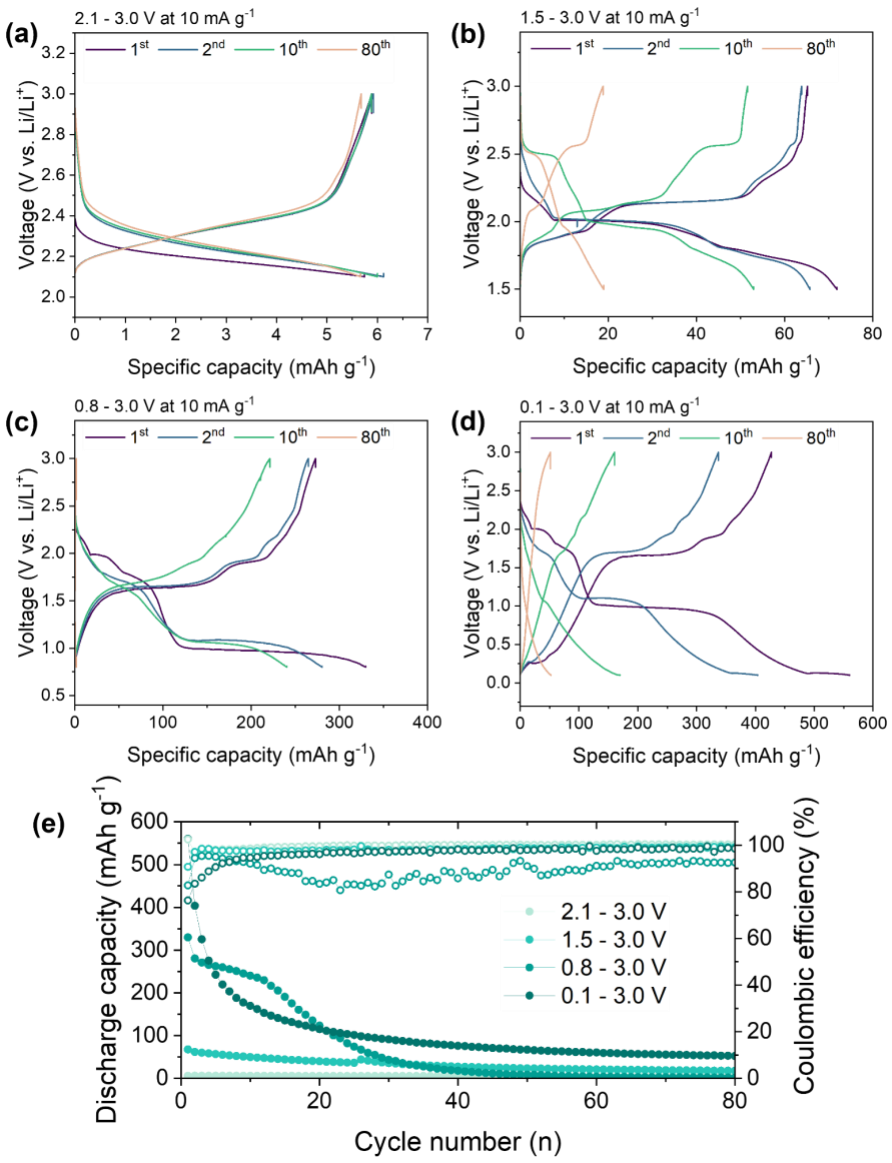

Figure S1. Evolution of the GCD curves at 10 mA/g for the 1st, 2nd, 10th, and 80th cycles within cutoff voltages of (a) 2.1 V, (b) 1.5 V, (c) 0.8 V, and (d) 0.1–3.0 V, showing progressive increases in voltage hysteresis and capacity loss with deeper discharge. (e) Long-term cycling at 10 mA g^{-1} for 80 cycles under each cutoff condition demonstrates that reversibility is highest at shallow cutoff and decreases substantially with deeper discharge.

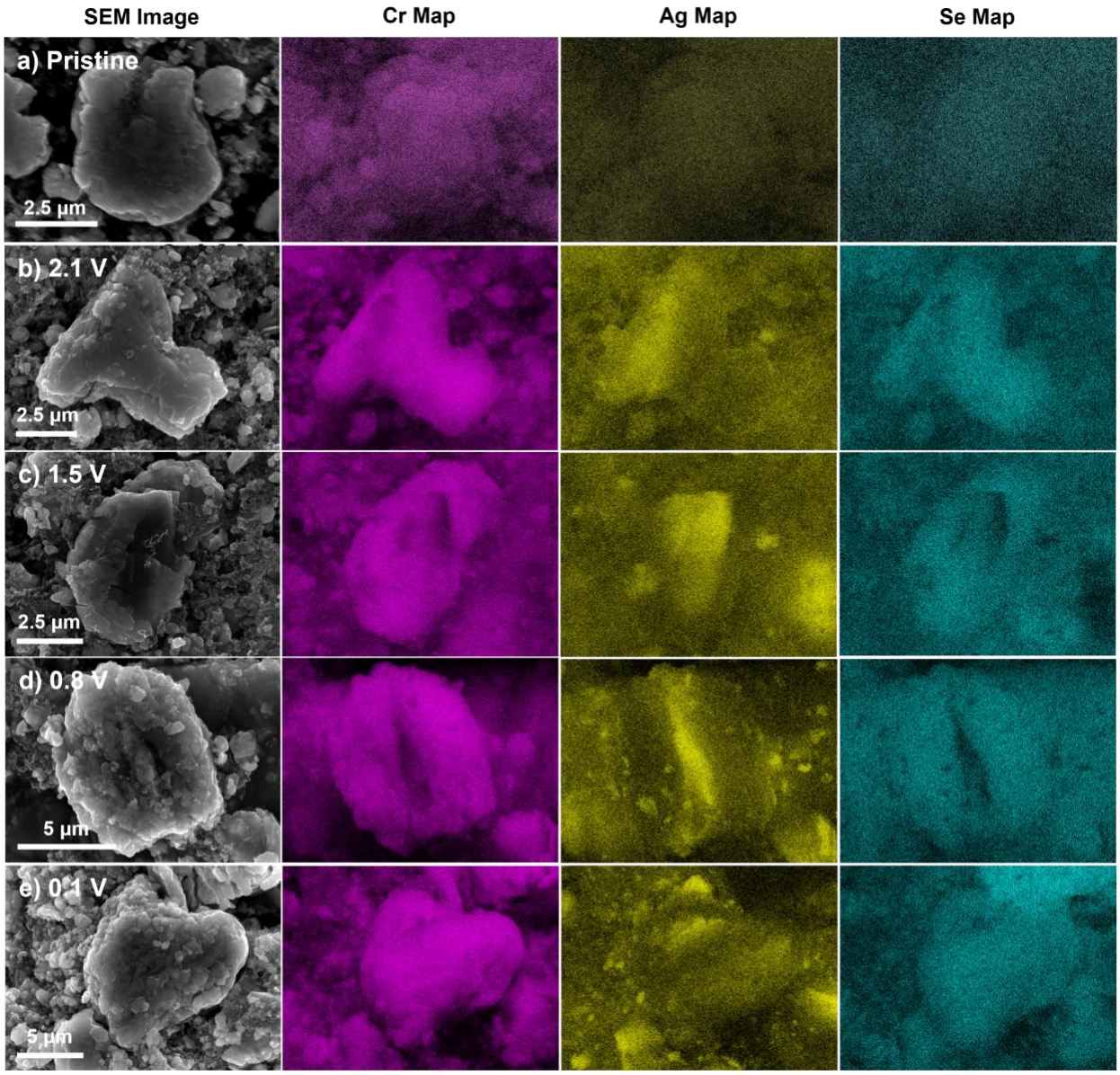

Figure S2. Ex situ SEM images of $AgCrSe_2$ particles and corresponding EDS maps of Cr, Ag, and Se (from left to right) for electrodes discharged to different cutoff voltages: (a) pristine, (b) 2.1 V, (c) 1.5 V, (d) 0.8 V, and (e) 0.1 V, showing the progressive redistribution of Ag and the emergence of localized Ag-rich regions with deeper discharge.

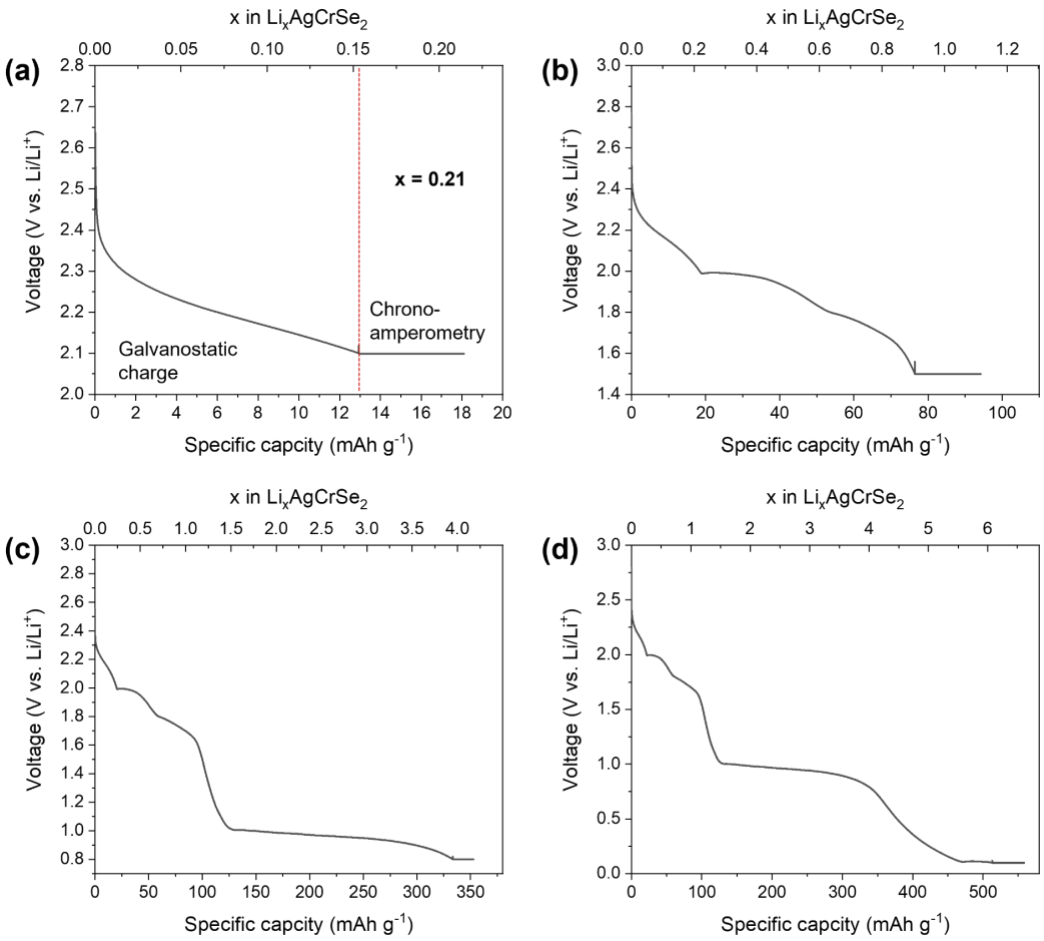

Figure S3. Example of the electrochemical protocol used to prepare ex situ samples at (a) 2.1 V, (b) 1.5 V, (c) 0.8 V, and (d) 0.1–3.0 V. The electrode was galvanostatically discharged to each target potential, followed by chronoamperometry until the potential stabilized at the corresponding cut-off voltage.

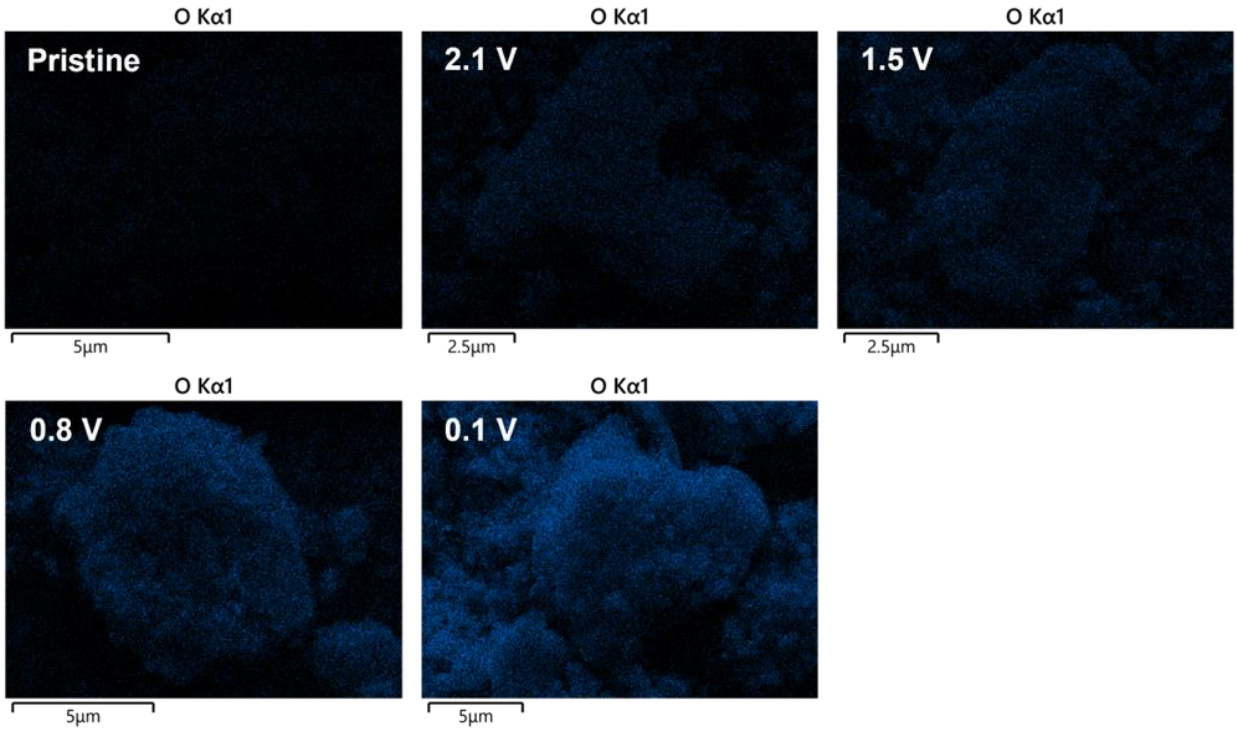

Figure S4. Ex situ EDS maps of oxygen in $AgCrSe_2$ electrodes reduced to different cutoff voltages: pristine, 2.1 V, 1.5 V, 0.8 V, and 0.1 V, showing increasing oxygen signal intensity with deeper lithiation, consistent with higher reactivity of the more reduced samples upon brief air exposure.

Table S1. Elemental composition (atomic %) of discharged electrodes at different cutoff voltages, as determined by ex-situ EDS analysis.

At.%	Pristine	2.1 V	1.5 V	0.8 V	0.1 V
C	72.6	74	73.3	56.7	59.2
O	2.1	2.7	3.9	10.9	16.9
Ag	5.9	4.1	3.6	4.8	2.9
Cr	6.3	4.5	3.5	6.9	4.8
Se	9.6	7.9	6.7	10.9	8.5
F	2.2	6.3	8.4	7.9	6.9
Cu	1.3	0.4	0.3	1.8	0.7
Cl	0.0	0.1	0.2	0.1	0.2

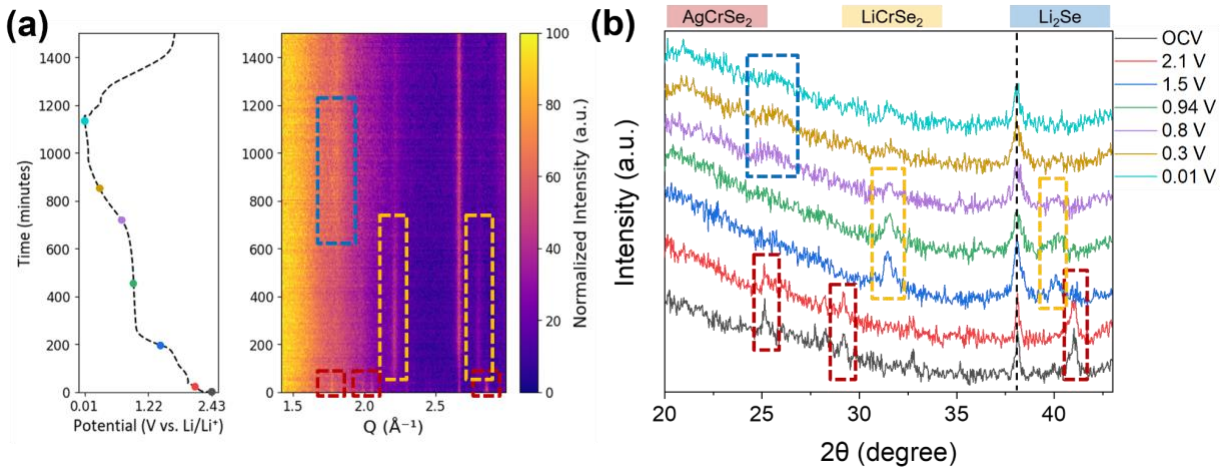

Figure S5. Operando electrochemical XRD of $AgCrSe_2$. Peaks marked with red squares correspond to $AgCrSe_2$, yellow squares to $LiCrSe_2$, and blue squares to Li_2Se. (a) Contour plot of operando XRD patterns during the first discharge, showing the sequential disappearance of $AgCrSe_2$ and emergence of $LiCrSe_2$ and Li_2Se. (b) Selected patterns highlighting the phase evolution with discharge.

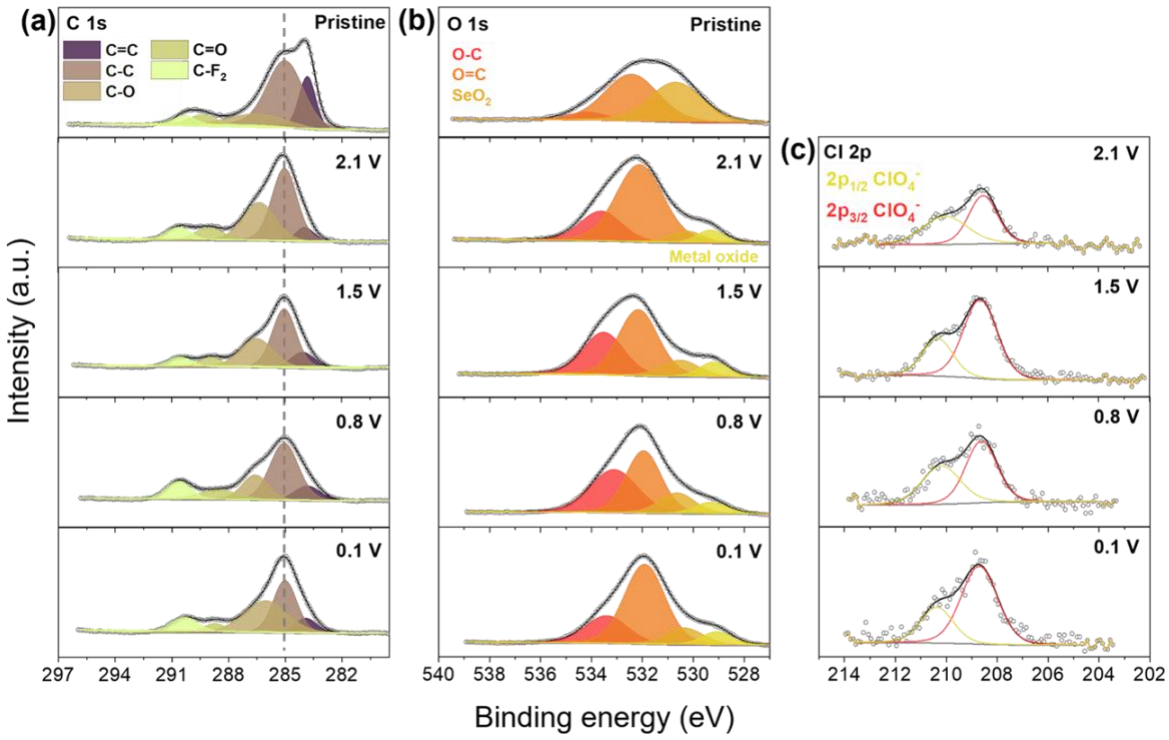

Figure S6. Evolution of (a) C 1s, (b) O 1s, and (c) Cl 2p spectra of $AgCrSe_2$ electrodes reduced to different cutoff voltages: pristine, 2.1, 1.5, 0.8, and 0.1 V, showing weakening of C=C and growth of C–O/C=O features due to electrolyte introduction on the surface, enhancement of O–C signals, and the appearance of Cl peaks confirming ClO^{4-} incorporation.

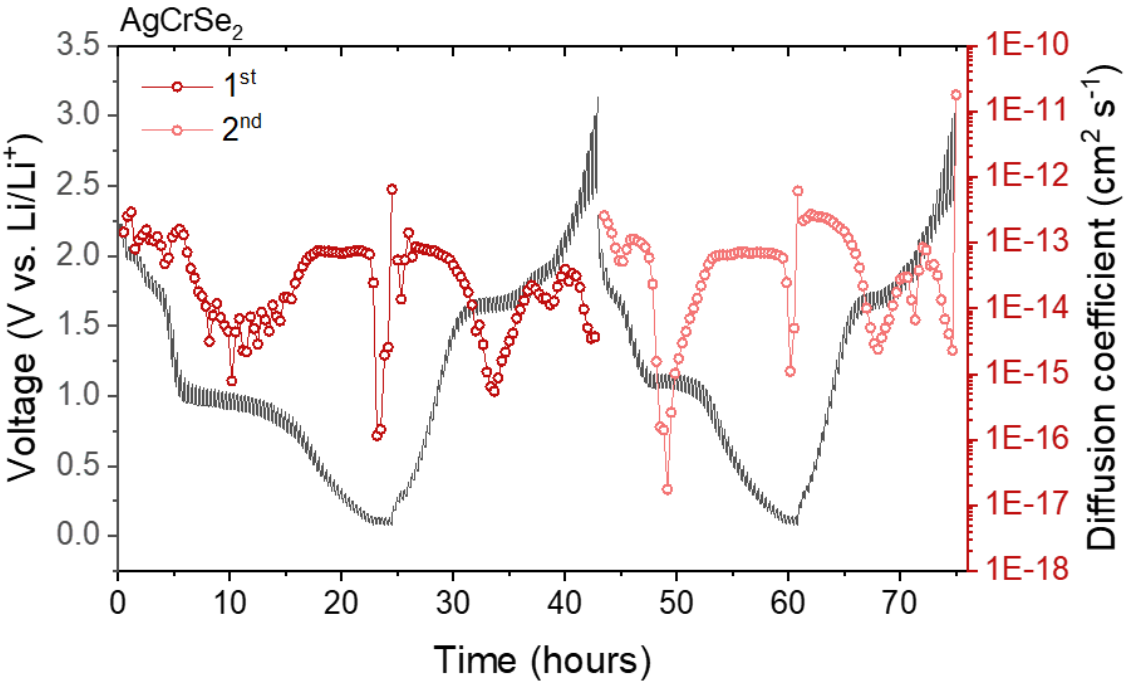

Figure S7. GITT analysis of an $AgCrSe_2$ electrode showing the stepwise potential response (left) and the corresponding apparent diffusion coefficient (right) during lithiation and delithiation in the potential range of 3.0–0.1 V, with diffusivity fluctuating but overall decreasing in Region I.

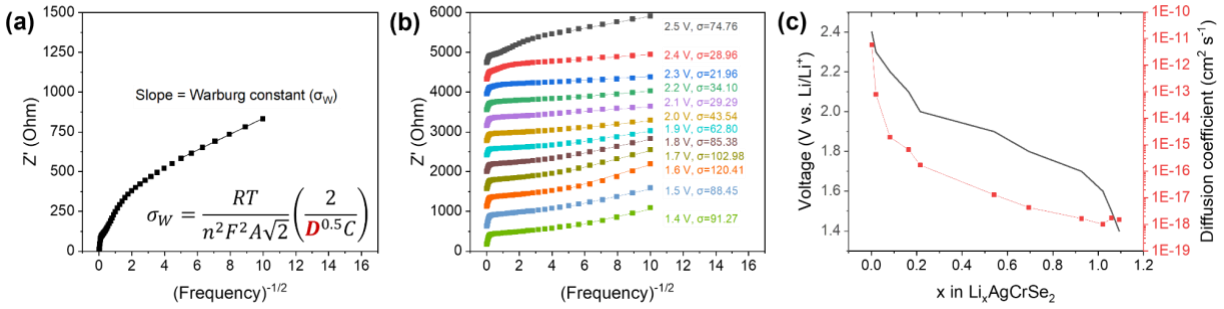

Figure S8. Electrochemical impedance analysis during the reduction of $AgCrSe_2$ from 2.5 to 1.4 V. (a) Example showing the linear fitting of Z' versus (frequency)$^{-1/2}$, including the slope corresponding to the Warburg constant (σ_W) and the equation used for calculating the diffusion coefficient. (b) Z' versus (frequency)$^{-1/2}$ plots at different voltages with their linear fittings. (c) Diffusion coefficient calculated from σ_W as a function of x in $Li_xAgCrSe_2$.

Table S2. Refined lattice parameters and R-factors of $AgCrSe_2$ and $CuCrSe_2$ obtained from Rietveld refinement.

Compound	Space group	a (Å)	c (Å)	Volume (Å^3)	R_{wp} (%)	R_p (%)	R_{exp} (%)
$AgCrSe_2$	R3m (No.160)	3.6804(1)	21.2170(7)	248.88(2)	1.90	1.23	1.08
$CuCrSe_2$	R3m (No.160)	3.6760(3)	19.3854(2)	226.865(4)	1.54	1.11	0.99

Table S3. Atomic positions and isotropic displacement parameters (B_{iso}) for $AgCrSe_2$ and $CuCrSe_2$.

Compound	Atom	x	y	z	Occ	B_{iso} (Å^2)
$AgCrSe_2$	Cr1	0	0	-0.0015(2)	1.00	3.36(3)
	Ag1	0	0	0.1473(1)	1.00	3.22(2)
	Se1	0	0	0.2650(1)	1.00	1.73(2)
	Se2	0	0	0.7312(1)	1.00	1.73(2)
$CuCrSe_2$	Cr1	0	0	0.0114(1)	1.00	1.09(5)
	Cu1	0	0	0.1567(1)	1.00	2.75(5)
	Se1	0	0	0.2754(1)	1.00	0.74(4)
	Se2	0	0	0.7542(1)	1.00	0.74(4)